ISSN 1674-1056
http://cpb.iphy.ac.cn
http://iopscience.iop.org/cpb
中国物理 B
Chinese Physics
中国物理 Chinese Physics B

Up-conversion luminescence tuning in Er^{3+}-doped ceramic glass by femtosecond laser pulse at different laser powers

Wen-Jing Cheng(程文静), Guo Liang(梁果), Ping Wu(吴萍), Shi-Hua Zhao(赵世华), Tian-Qing Jia(贾天卿), Zhen-Rong Sun(孙真荣), Shi-An Zhang(张诗按)

Citation:CChin. Phys. B . 2018, 27(12): 123201. **doi:** 10.1088/1674-1056/27/12/123201
Journal homepage: http://cpb.iphy.ac.cn; http://iopscience.iop.org/cpb

What follows is a list of articles you may be interested in

Simulating resonance-mediated two-photon absorption enhancement in rare-earth ions by a rectangle phase modulation

Da-Long Qi(齐大龙), Ye Zheng(郑烨), Wen-Jing Cheng(程文静), Yun-Hua Yao(姚云华), Lian-Zhong Deng(邓联忠), Dong-Hai Feng(冯东海), Tian-Qing Jia(贾天卿), Zhen-Rong Sun(孙真荣), Shi-An Zhang(张诗按)

Chin. Phys. B . 2018, 27(1): 013202. **doi:** 10.1088/1674-1056/27/1/013202

Up-conversion luminescence polarization control in Er^{3+}-doped $NaYF_4$ nanocrystals

Hui Zhang(张晖), Yun-Hua Yao(姚云华), Shi-An Zhang(张诗按), Chen-Hui Lu(卢晨晖), Zhen-Rong Sun(孙真荣)

Chin. Phys. B . 2016, 25(2): 023201. **doi:** 10.1088/1674-1056/25/2/023201

On-chip optical pulse shaper for arbitrary waveform generation

Liao Sha-Sha, Yang Ting, Dong Jian-Ji

Chin. Phys. B . 2014, 23(7): 073201. **doi:** 10.1088/1674-1056/23/7/073201

Diversity of photonic differentiators based on flexible demodulation of phase signals

Zheng Ao-Ling, Dong Jian-Ji, Lei Lei, Yang Ting, Zhang Xin-Liang

Chin. Phys. B . 2014, 23(3): 033201. **doi:** 10.1088/1674-1056/23/3/033201

Polarization and phase control of two-photon absorption in an isotropic molecular system

Lu Chen-Hui, Zhang Hui, Zhang Shi-An, Sun Zhen-Rong

Chin. Phys. B . 2012, 21(12): 123202. **doi:** 10.1088/1674-1056/21/12/123202

Up-conversion luminescence tuning in Er^{3+}-doped ceramic glass by femtosecond laser pulse at different laser powers*

Wen-Jing Cheng(程文静)[1,†], Guo Liang(梁果)[1], Ping Wu(吴萍)[1], Shi-Hua Zhao(赵世华)[1], Tian-Qing Jia(贾天卿)[2], Zhen-Rong Sun(孙真荣)[2], and Shi-An Zhang(张诗按)[2,‡]

[1] *School of Electronic & Electrical Engineering, Shangqiu Normal University, Shangqiu* 476000, *China*
[2] *State Key Laboratory of Precision Spectroscopy, East China Normal University, Shanghai* 200062 *China*

(Received 23 August 2018; revised manuscript received 26 September 2018; published online 10 November 2018)

The up-conversion luminescence tuning of rare-earth ions is an important research topic for understanding luminescence mechanisms and promoting related applications. In this paper, we experimentally study the up-conversion luminescence tuning of Er^{3+}-doped ceramic glass excited by the unshaped, V-shaped and cosine-shaped femtosecond laser field with different laser powers. The results show that green and red up-conversion luminescence can be effectively tuned by varying the power or spectral phase of the femtosecond laser field. We further analyze the up-conversion luminescence tuning mechanism by considering different excitation processes, including single-photon absorption (SPA), two-photon absorption (TPA), excited state absorption (ESA), and energy transfer up-conversion (ETU). The relative weight of TPA in the whole excitation process can increase with the increase of the laser power, thereby enhancing the intensity ratio between green and red luminescence (I_{547}/I_{656}). However, the second ETU (ETU2) process can generate red luminescence and reduce the green and red luminescence intensity ratio I_{547}/I_{656}, while the third ESA (ESA3) process can produce green luminescence and enhance its control efficiency. Moreover, the up-conversion luminescence tuning mechanism is further validated by observing the up-conversion luminescence intensity, depending on the laser power and the down-conversion luminescence spectrum under the excitation of 400-nm femtosecond laser pulse. These studies can present a clear physical picture that enables us to understand the up-conversion luminescence tuning mechanism in rare-earth ions, and can also provide an opportunity to tune up-conversion luminescence to promote its related applications.

Keywords: rare-earth ions, up-conversion luminescence, pulse shaping, two-photon absorption

PACS: 32.80.Qk, 32.80.Wr, 61.46.Hk **DOI:** 10.1088/1674-1056/27/12/123201

1. Introduction

The up-conversion luminescence of rare-earth ions is a nonlinear optical phenomenon, which can absorb low-energy excitation light and produce high-energy ultraviolet or visible emission. This phenomenon has been extensively explored because of its distinct optical properties, such as near infrared excitation, photostability, narrow spectrum, large Stokes shift, long luminescence lifetime, and well-defined emission bands.[1,2] Recently, the up-conversion luminescence of rare-earth ions has widely applied in many fields, such as laser sources,[3,4] fiber-optic communications,[5,6] light-emitting diodes,[7] solar cells,[8] color displays,[9,10] biolabeling and biomedical sensors.[11–15] The up-conversion luminescence mechanism of rare-earth ions can be changed by exciting different light sources. When the rare-earth ions are excited by the continuous wave laser, the ground state absorption (GSA) or excited state absorption (ESA),[16,17] energy transfer up-conversion (ETU),[18] and photon avalanche (PA)[19] are important up-conversion luminescence processes among numerous fundamental mechanisms. A femtosecond laser field has a high peak intensity and a short pulse duration. It also easily excites the up-conversion luminescence of rare-earth ions through two-photon absorption (TPA) or multi-photon absorption (MPA).[20,21]

In recent years, realizing the up-conversion luminescence tuning of rare-earth ions has become a popular research topic and is very important for promoting its relevant applications. For example, controllable red, green and blue emission can be used in the bright white emission and color display. Single-band up-conversion emission is applied to biomedical sensing images, and multiple color tuning is important for anti-counterfeiting applications. The relevant studies have proposed some methods to tune the up-conversion luminescence of rare-earth ions. For example, conventional chemical method can be utilized to effectively tune the up-conversion luminescence of rare-earth ions by changing chemical composition,[22] crystal structure,[23] nanoparticle size,[24] and surface groups.[25] Physical methods could

*Project supported by the National Natural Science Foundation of China (Grant Nos. 51132004, 11474096, 11604199, U1704145, and 11747101), the Fund from the Science and Technology Commission of Shanghai Municipality, China (Grant No. 14JC1401500), the Henan Provincial Natural Science Foundation, China (Grant No. 182102210117), and the Higher Educational Key Program of Henan Province of China (Gant Nos. 17A140025 and 16A140030).

†Corresponding author. E-mail: 0110wenjing@163.com
‡Corresponding author. E-mail: sazhang@phy.ecnu.edu.cn

© 2018 Chinese Physical Society and IOP Publishing Ltd

also be used to tune up-conversion luminescence of rare-earth ions, such as applying electric field,[26] magnetic field,[27] plasmon,[28] temperature,[29] and laser parameters.[30–33] In addition, our group has realized luminescence modulation by modulating the phase or polarization of the femtosecond laser field.[34,35] For example, the single-photon and two-photon luminescence in Er^{3+} ion can be enhanced or suppressed by π or square phase modulation.[34] The green and red up-conversion luminescence in Er^{3+}-doped $NaYF_4$ nanocrystals can be tuned by the square phase modulation.[35] However, up-conversion luminescence tuning by varying laser power or performing multiply spectral phase modulation is rarely studied because of the complexity and the coexistence of the multiple excitation processes.

In this paper, we propose a new scheme to tune the up-conversion luminescence in Er^{3+}doped ceramic glass by varying the power or spectral phase of the femtosecond pulse. The experimental results show that green and red up-conversion luminescence can be effectively tuned by varying the laser power of the unshaped or V-shaped femtosecond pulse, but cannot be modulated by modifying the laser power of the cosine-shaped femtosecond pulse. We explain the experimental observations by analyzing different excitation processes. The relative weight of TPA in the whole excitation processes can increase as the laser power increases, thereby increasing the intensity ratio between green and red luminescence (I_{547}/I_{656}). Moreover, the second ETU process suppresses the intensity ratio between green and red luminescence I_{547}/I_{656}, while the third ESA process can enhance the intensity ratio of I_{547}/I_{656}. The up-conversion luminescence tuning mechanism in Er^{3+}-doped ceramic glass is further validated by observing the up-conversion luminescence intensity at different laser powers and the down-conversion luminescence under 400-nm femtosecond laser pulse excitation.

2. Experiment

In our experiment, 5%Er^{3+}-doped $NaYF_4$ nanocrystals dispersed in silicate glass were used as our sample and were prepared with the composition of $40SiO_2$–$25Al_2O_3$–$18NaCO_3 10YF_3$–$7NaF$–$5ErF_3$ (in unit mol%). The mixed raw materials were placed in a platinum crucible with a lid, and were treated for 45 min at 1450 °C in an ambient atmosphere and successively heated at 450 °C for 10 h. Glass products were further processed by incising and polishing, and the sample with a size of 7 mm×12 mm×2.5 mm was used in our optical experiment. The x-ray diffraction (XRD) patterns and transition electron microscopy (TEM) images were obtained in accordance with previously described methods[36] to reveal the existence of a cubic α-NaYF4 crystal. Moreover, the spherical nanocrystals were distributed densely and homogeneously in a glass matrix with an average size of 20 nm–30 nm. Figure 1(a) shows the experimental arrangement to control the up-conversion luminescence of Er^{3+}-doped ceramic glass via the femtosecond pulse shaping method. A Ti:sapphire mode-locked laser was used as an excitation source, which can produce a femtosecond laser field with a pulse width of 50 fs, a central wavelength of 800 nm and a repetition rate of 1 kHz. The output laser was shaped by the zerodispersion programmable 4f configuration pulse shaping system, which is composed of two diffraction gratings (G_1 and G_2), two column concave mirrors (C_1 and C_2), three optical lenses (L_1, L_2, and L_3), and one spatial light modulator (SLM). Here, the SLM was used to modulate the phase or amplitude of the femtosecond laser field in frequency domain. Then, all of the luminescence signals emitted by the Er^{3+}-doped ceramic glass were collected and measured by using a spectrometer with a charge-coupled device.

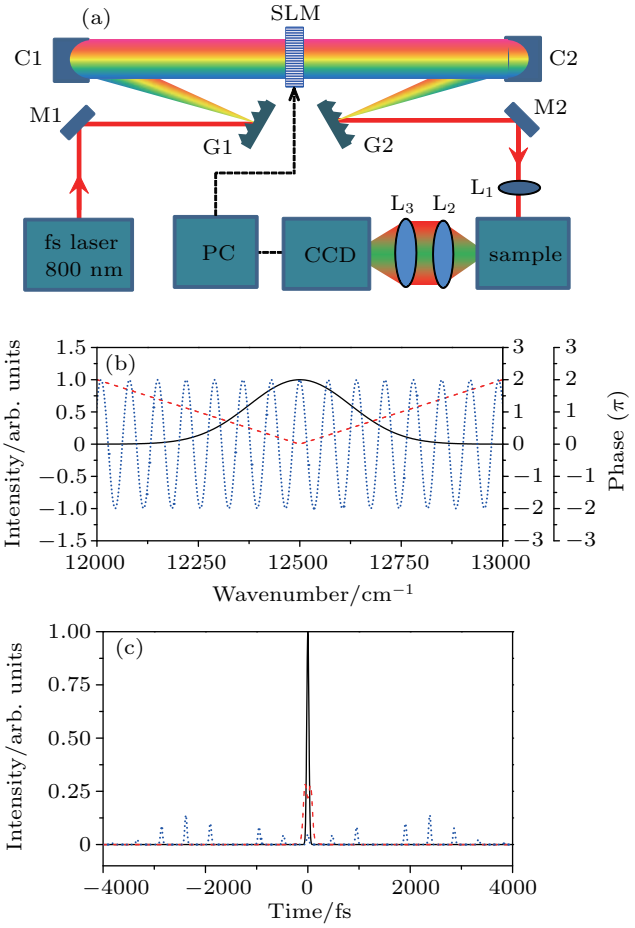


Fig. 1. (color online) (a) Experimental arrangement for controlling up-conversion luminescence in Er^{3+}-doped ceramic glass by femtosecond pulse shaping method, (b) laser spectrum (black solid line) modulated by V-style (red dashed line) and cosine phase (blue dotted line), (c) temporal intensity profile of the unshaped (black solid line), the V-shaped (red dashed line) and cosine-shaped (blue dotted line) femtosecond laser fields.

The femtosecond pulse shaping technique has been widely used to control multi-photon absorption in atomic and

molecular systems, and the V-style and cosine phase modulation have been utilized in actual experiments.[37,38] Here, we further utilize the V-style and cosine phase modulation to tune up-conversion luminescence of the Er^{3+}-doped ceramic glass. We show the laser spectrum (black solid line) and the V-style (red dashed line) and cosine phase (blue dotted line) modulation in Fig. 1(b), and their corresponding temporal intensity distributions in Fig. 1(c). As can be seen in Fig. 1(b), the full width at half maximum (FWHM) of the laser spectrum is 300 cm^{1}, and can effectively excite the TPA of Er^{3+} ions. The V-style phase modulation can be expressed by the function of $\Phi(\omega) = \tau|\omega - \omega_0 - \delta\omega|$, where τ and $\delta\omega$ are the phase modulation depth and the modulation position, respectively. The cosine phase modulation can be defined by the function of $\Theta(\Omega) = \alpha\cos(\beta\Omega + \varphi)$, where α, β, and φ are the depth, frequency, and phase of the modulation, respectively. Moreover, the modulation frequency β can be expressed by the function of $\beta = 2\pi/\Delta$. Based on the experiment conditions, the phase modulation depth τ and position $\delta\omega$ are set to be π and 0 for the V-style phase modulation, while α, Δ, and φ are set to be 2π, 70 cm^{-1}, and 0 for the cosine phase modulation. As shown in Fig. 1(c), the single laser pulse (*i.e.*, unshaped femtosecond laser pulse) is divided into two subpulses by the V-style phase modulation. By contrast, the single laser pulse is transformed into multiple subpulses via the cosine phase modulation. Obviously, the peak intensity of cosine-shaped femtosecond pulse is lower than that of the unshaped or V-shaped femtosecond pulse. The laser repetition rate is 1 kHz, and the laser pulse separation is 1 ms, which is longer than the excited state lifetime of Er^{3+} ion in a range of microseconds. Therefore, only one unshaped or shaped femtosecond pulse can survive in the range of the excited state lifetime.

3. Results and discussion

The UV-Vis-NIR absorption spectrum of the Er^{3+}-doped ceramic glass is shown in Fig. 2(a), which is obtained with a U4100 spectrophotometer (Hitachi). As can be seen, there are eight main absorption bands that correspond to these excited states $^4I_{9/2}$, $^4F_{9/2}$, $^4S_{3/2}$, $^2H_{11/2}$, $^4F_{7/2}$, $^4F_{3/2}$, $^2H_{9/2}$, and $^4G_{11/2}$. Clearly, an obvious absorption peak at a wavelength of 796 nm can be observed. Moreover, we show the up-conversion luminescence spectrum of the Er^{3+}-doped ceramic glass excited by the unshaped (Fig. 2(b)), the V-shaped (Fig. 2(c)), and cosine-shaped (Fig. 2(d)) femtosecond laser field with the laser power of 19 mW (black solid line), 39 (red dashed line), 51 mW (blue dotted line), and 63 mW (green dashed–dotted line), respectively. The red and green up-conversion luminescences in the visible light region can be clearly observed. Three up-conversion luminescence signals at wavelengths of 656, 527, and 547 nm can be attributed to the transition processes of $^4F_{9/2} \rightarrow {}^4I_{15/2}$, $^4S_{3/2} \rightarrow {}^4I_{15/2}$, and $^2H_{11/2} \rightarrow {}^4I_{15/2}$, respectively. Moreover, as can be seen in Figs. 2(b), 2(c), and 2(d), the up-conversion luminescence intensity of the Er^{3+}-doped ceramic glass increases with the laser power increasing but the spectral shapes and locations remain unchanged under the different laser powers, which illustrates that neither is the color center changed nor are the other luminescence processes involved.

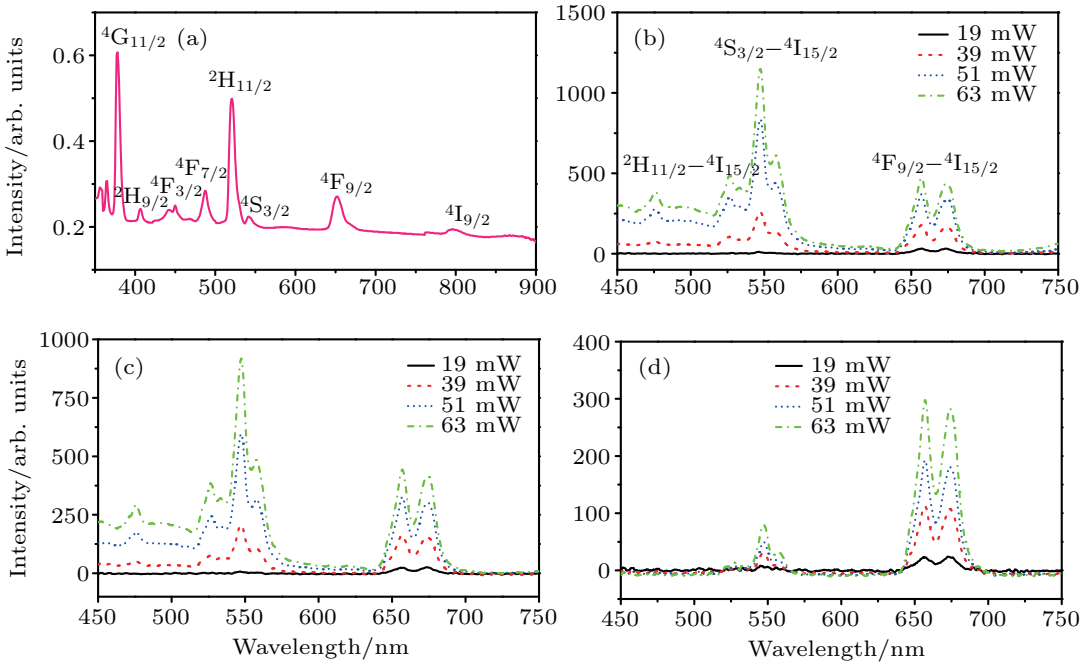


Fig. 2. (color online) (a) UV-Vis-NIR absorption spectrum of the Er^{3+}-doped ceramic glass, and up-conversion luminescence spectra excited by (b) unshaped, (c) V-shaped, and (d) cosine-shaped femtosecond laser fields respectively with laser powers of 19 (black solid line), 39 (red dashed line), 51 (blue dotted line), and 63 mW (green dashed–dotted line).

In the experiment, we use the unshaped, V-shaped and cosine-shaped femtosecond laser pulse to excite the Er^{3+}-doped ceramic glass, and we collect the up-conversion luminescence signals by a spectrometer, and further observe and analyze the intensity ratio between green and red up-conversion luminescence under different laser powers. Figure 3 shows the intensity ratio between green (547 nm) and red (656 nm) luminescence (I_{547}/I_{656}) by varying the laser power of the unshaped (olive squares), V-shaped (red circles), and cosine-shaped (blue triangles) femtosecond laser pulse. As can be seen, the intensity ratio of I_{547}/I_{656} can be effectively tuned by varying the laser power of the unshaped and V-shaped femtosecond laser pulse, and the intensity ratio of I_{547}/I_{656} for unshaped femtosecond laser pulse can increase more quickly than that of the V-shaped femtosecond laser pulse. However, for the cosine-shaped femtosecond laser pulse, the intensity ratio of I_{547}/I_{656} is almost unchanged when varying the laser power. Moreover, at the same higher laser power, the intensity ratio of I_{547}/I_{656} changes when using the unshaped, V-shaped and cosine-shaped femtosecond laser pulse separately. Therefore, one can conclude that the intensity ratio of I_{547}/I_{656} can be effectively tuned by varying the power or spectral phase of the femtosecond laser field.

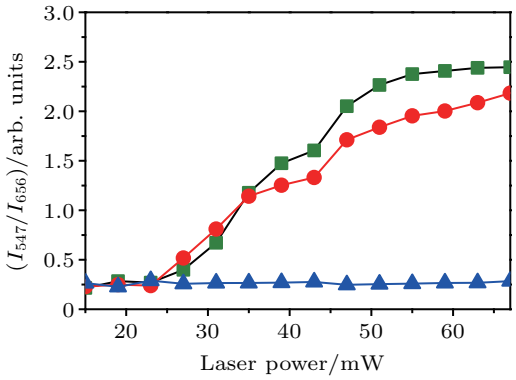


Fig. 3. (color online) The plots of intensity ratio between green (547 nm) and red (656 nm) up-conversion luminescence I_{547}/I_{656} *versus* laser power modulated with unshaped (olive squares), V-shaped (red circles), and cosine-shaped (blue triangles) femtosecond laser fields.

To demonstrate the physical mechanism of the green and red up-conversion luminescence tuning by varying the laser power or spectral phase, we show the energy level diagram of Er^{3+} ion and the possible excitation and emission processes in Fig. 4. As can be seen in Fig. 4(a), for the unshaped or V-shaped femtosecond laser pulse, the population in the ground state $^4I_{15/2}$ can be pumped to the excited state $^4I_{9/2}$ by the SPA. The femtosecond laser field has a relatively wide spectrum bandwidth (FWHM) of 300 cm^{-1}, the intermediate state $^4I_{9/2}$ with the transition frequency of 12563 cm^{-1} (796 nm) is within the laser spectral range, and the excitation state $^2H_{9/2}$ can be populated by a resonant-mediated two-photon absorption (TPA).[39] Then, the population in the excited state $^2H_{9/2}$ can spontaneously decay to the excited states $^2H_{11/2}$, $^4S_{3/2}$, and $^4F_{9/2}$, and further emits the green and red up-conversion luminescence with the wavelengths of 527, 547, and 656 nm, respectively. At a high dopant concentration of Er^{3+} ions, the neighboring Er^{3+} ions have a small average distance, and the ETU always occurs. The population in the excited state $^4I_{9/2}$ can spontaneously decay to the lower excited states $^4I_{11/2}$ and $^4I_{13/2}$, and further pump to the higher excited states $^4F_{7/2}$ and $^4F_{9/2}$ via ETU1 and ETU2, and generate the green and red up-conversion luminescence. Compared with the unshaped and V-shaped femtosecond pulses, the cosine-shaped femtosecond pulse has multiple subpulses within the excited state lifetime. As can be seen in Fig. 4(b), for the cosine-shaped femtosecond pulse, except the SPA, TPA, and ETU processes, the population in excited states $^4I_{9/2}$, $^4I_{11/2}$, $^4I_{13/2}$ can be pumped to the higher excited states $^2H_{9/2}$, $^4F_{3/2}$, and $^4S_{3/2}$ by ESA1, ESA2, and ESA3, and further generate the green and red up-conversion luminescence. Therefore, the green up-conversion luminescence can be obtained through TPA, ETU1, ESA1, ESA2, and ESA3, while the red up-conversion luminescence can be generated by the processes of TPA, ETU1, ETU2, ESA1, and ESA2. Obviously, the red luminescence generation additionally contain the ETU2 process, while the green luminescence generation additionally contains the ESA3 process.

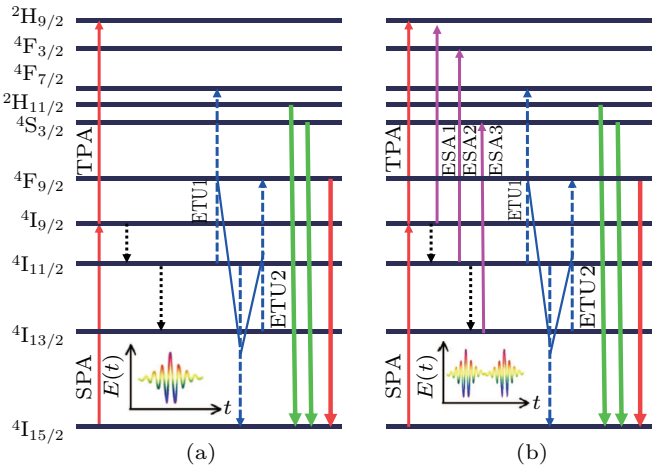


Fig. 4. (color online) Energy level diagram of Er^{3+} ions and the possible up-conversion processes for green and red luminescence generations by (a) unshaped and the V-shaped and (b) cosine-shaped femtosecond laser pulse.

Since the generation of red and green luminescence can be attributed to different excited pathways for the unshaped and shaped femtosecond pulses, we can explain the green and red up-conversion luminescence tuning in Fig. 3 by analyzing TPA, ESA, and ETU process. As can be seen from Figs. 4(a) and 4(b), the intensity ratio of I_{547}/I_{656} by the TPA, ETU1, ESA1, and ESA2 should be the same for the spontaneous decay from the higher excited states $^2H_{9/2}$, $^4F_{7/2}$, and $^4F_{3/2}$, which correspond to a higher intensity ratio between green and red up-conversion luminescence. However, ETU2 process can generate the red luminescence and reduce the intensity ratio of

I_{547}/I_{656}, while the ESA3 process can produce the green luminescence and enhance its control efficiency. Moreover, the up-conversion luminescence by the ESA and ETU process are correlated with the population of the excited states $^4I_{9/2}$, $^4I_{11/2}$ or $^4I_{13/2}$ by the SPA process, while the up-conversion luminescence by the TPA is related to the population of the excited state $^2H_{9/2}$. Therefore, the up-conversion luminescence intensities depending on the laser power of ESA, ETU, and SPA are similar, but different from that of TPA.

We first demonstrate the physical mechanism of green and red up-conversion luminescence tuned by varying the laser power of the unshaped and V-shaped femtosecond pulse. For the unshaped femtosecond laser pulse, under the lower laser power, the TPA cannot effectively occur. The green luminescence is mainly generated by the ETU1 process, while the red luminescence is mainly contributed by the ETU1 and ETU2 process, which leads to the lower intensity ratio of I_{547}/I_{656}. However, under the higher laser power, the TPA can be effectively excited, which plays an important role in generating the green and red luminescence. With the increase of the laser power, the relative weight of the TPA in the whole excitation process can be increased, which induces the intensity ratio of I_{547}/I_{656} to rise. Comparing with the unshaped femtosecond laser pulse, the peak intensity of the V-shaped femtosecond pulse is weak but it is still larger than that of the cosine-shaped femtosecond pulse. The relative weight of TPA in the whole excitation process for the V-shaped femtosecond pulse is lower than that for unshaped femtosecond pulse under the same laser power. Consequently, the intensity ratio of I_{547}/I_{656} for the V-shaped femtosecond pulse is lower than that of unshaped femtosecond laser pulse. Therefore, the intensity ratio tuning of I_{547}/I_{656} by varying the laser power for the unshaped or V-shaped femtosecond pulse can be attributed mainly to the change in the relative weight of TPA in the whole excitation process.

We further analyze the influence of laser power on the intensity ratio of I_{547}/I_{656} for the cosine-shaped femtosecond pulse. Compared with the unshaped femtosecond pulse and V-shaped femtosecond pulses, the cosine-shaped femtosecond pulse has multiple subpulses, and its peak intensity is very weak. Even when the laser power is increased, the TPA still cannot be effectively excited. The ESA and ETU process can occur but their relatively weight remains unchanged as the laser power varies. Moreover, it is clear that the ESA3 process can enhance the green luminescence, while the ETU2 process can enhance the red luminescence. By varying the laser power of the cosine-shaped femtosecond pulse, the green and red luminescence generation can simultaneously change, resulting in a nearly constant intensity ratio of I_{547}/I_{656}. Therefore, the intensity ratio tuning of I_{547}/I_{656} by varying the laser power for cosine-shaped femtosecond pulse can be attributed to the stable relative weight of ESA and ETU process in the whole process.

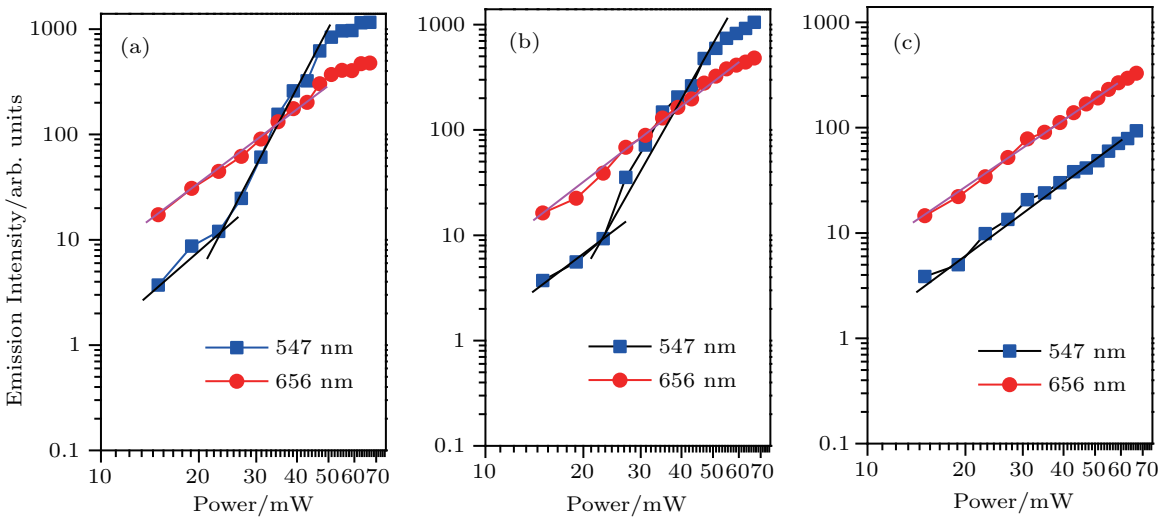


Fig. 5. (color online) Plots of green (blue squares) and red (red circles) up-conversion luminescence of the Er^{3+}-doped ceramic glass by varying laser power of (a) unshaped, (b) V-shaped, and (c) cosine-shaped femtosecond laser field.

To further verify our findings about the mechanisms for the green up-conversion luminescence and the red up-conversion luminescence, respectively, we show the up-conversion luminescence intensity at wavelengths of 547 nm (blue squares) and 656 nm (red circles) by varying the laser power of the unshaped (Fig. 5(a)), V-shaped (Fig. 5(b)), and cosine-shaped (Fig. 5(c)) femtosecond laser field in Fig. 5. When the laser power is larger than 55 mW, the up-conversion luminescence is saturated. We analyze the luminescence experimental data of the lower and higher laser intensities indicated by three solid lines with different slopes. As can be seen in Figs. 5(a) and 5(b), for the unshaped and V-shaped femtosecond laser field, the slope of the green up-conversion luminescence under a lower laser power is smaller than that

of the red up-conversion luminescence but is larger at a higher laser power. This can be explained as follows. The contribution of TPA to the whole excitation process is smaller at a lower laser power but its contribution can increase as the laser power increases, which induces the slope of the green up-conversion luminescence to increase. However, as can be seen in Fig. 5(c), the slope of the green up-conversion luminescence is similar to that of the red up-conversion luminescence for the cosine-shaped femtosecond laser field. By the cosine-shaped modulation, the peak of the multiple subpulses decreases, and the TPA cannot be effectively excited by increasing the laser power.

To further verify the important role of TPA in green and red up-conversion luminescence, we use a 400-nm femtosecond pulse to excite the Er^{3+}-doped ceramic glass to simulate the TPA. The down-conversion luminescence spectrum in the visible light region is shown in Fig. 6. The green and red luminescence can be observed in the visible light region, and the intensity of the green luminescence is higher than that of the red luminescence, which corresponds to the higher intensity ratio of I_{547}/I_{656}. It is obvious that the TPA can play an important role in generating the green and red up-conversion luminescence, and the increase of the relative weight of TPA in the whole excitation process can induce the intensity ratio I_{547}/I_{656} to increase.

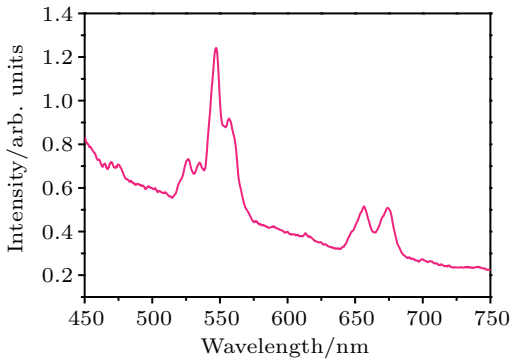


Fig. 6. (color online) Down-conversion luminescence spectrum in visible light region, obtained by 400-nm femtosecond laser pulse excitation.

According to these studies, we can find that the unshaped or the V-shaped pulse has an ultrashort pulse duration, and does not induce the ESA process, while the cos-shaped pulse with multiple subpulses can effectively excite the higher excited state absorption by the ESA process. By increasing the laser power, the relative weight of the TPA in the whole excited process can increase for the unshaped and V-shaped femtosecond pulse, while the TPA cannot be effective excited for cos-shaped femtosecond pulse. Therefore, the multiple time-delayed subpulses can create the ESA process and the larger laser power can induce the effective TPA in rare-earth ions. These femtosecond pulse shaping techniques can be further extended to tune the up-conversion luminescence of other rare-earth doped nanomaterials

4. Conclusions

In this work, we have tuned the intensity ratio between the green and red up-conversion luminescence of Er^{3+}-doped ceramic glass by varying the laser power of unshaped, V-shaped and cosine-shaped femtosecond laser pulse. The experimental results show that the intensity ratio between green and red up-conversion luminescence can be increased by increasing the laser power of the unshaped and V-shaped femtosecond field, while it is nearly unchanged by varying the laser power of the cosine-shaped femtosecond field. Our analysis indicates that the increase of the relative weight of TPA in the whole excitation process can increase the intensity ratio of I_{547}/I_{656}, the ETU2 process can generate the red up-conversion luminescence and reduce the intensity ratio of I_{547}/I_{656}, while the ESA3 process can produce the green up-conversion luminescence and enhance its control efficiency. These studies present a clear physical picture of the green and red up-conversion luminescence tuning in rare-earth ions and they can also provide a new way to control the up-conversion luminescence tuning of rare-earth ions. Future studies can design the experiment from two aspects to tune the intensity ratio of green and red up-conversion luminescence: the first is to control the power of a femtosecond laser field, and the second is to modulate the spectral phase of a femtoseocond laser pulse.

References

[1] Auzel F 2004 *Chem. Rev.* **104** 139
[2] Wang F and Liu X 2009 *Chem. Soc. Rev.* **38** 976
[3] Nilsson J, Clarkson W A, Selvas R, Sahu J K, Turner P W, Alam S U and Grudinin A B 2004 *Opt. Fiber. Technol.* **10** 5
[4] Wintner E, Sorokin E and Sorokina I T 2001 *Laser Phys.* **11** 1193
[5] Tessler N, Medvedev V, Kazes M, Kan S and Banin U 2002 *Science* **295** 1506
[6] Zhou P, Wang X, Ma Y, Lü H and Liu Z 2012 *Laser Phys.* **22** 1744
[7] Sivakumar S, Veggel F C J M and Raudsepp M 2005 *J. Am. Chem. Soc.* **127** 12464
[8] Wang H Q, Batentschuk M, Osvet A, Pinna L and Brabec C J 2011 *Adv. Mater.* **23** 2675
[9] Downing E, Hesselink L, Ralston J and Macfarlane R 1996 *Science* **273** 1185
[10] Li Y, Zhang J, Luo Y, Zhang X and Hao Z 2011 *J. Mater. Chem.* **21** 2895
[11] Nyk M, Kumar R, Ohulchanskyy T Y, Bergey E J and Prasad P N 2008 *Nano. Lett.* **8** 3834
[12] Wang F, Tan W B, Zhang Y, Fan X and Wang M 2006 *Nanotechnology* **17** R1
[13] Yu M, Li F, Chen Z, Hu H, Zhan C, Yang H and Huang C 2009 *Anal. Chem.* **81** 930
[14] Vetrone F, Naccache R, Zamarron A, Fuente A J, Sanz-Rodriguez F, Maestro L M, Rodriguez E M, Jaque D, Sole J G and Capobianco J A 2010 *ACS Nano* **4** 3254
[15] Gai S, Li C, Yang P and Lin J 2014 *Chem. Rev.* **114** 2343
[16] Scheps R 1996 *Prog. Quantum Electron.* **20** 271
[17] Piatkowski D and Mackowski S 2012 *Opt. Mater.* **34** 2055

[18] Wright J C 1976 *Up-conversion and excited state energy transfer in rare-earth doped materials* (Springer) pp. 239–295
[19] Joubert M 1999 *Opt. Mater.* **11** 181
[20] Deng R, Qin F, Chen R, Huang W, Hong M and Liu X 2015 *Nat. Nanotechnol.* **10** 237
[21] Bettinelli M 2015 *Nat. Nanotechnol.* **10** 203
[22] Wang F and Liu X 2008 *J. Am. Chem. Soc.* **130** 5642
[23] Teng X, Zhu Y, Wei W, Wang S, Huang J, Naccache R, Hu W, Iing A, Tok Y, Han Y, Zhang Q, Fan Q, Huang W, Capobianco J A and Huang L 2012 *J. Am. Chem. Soc.* **134** 8340
[24] Yuan D, Tan M C, Riman R E and Chow G M 2013 *J. Phys. Chem. C* **117** 13297
[25] Yuan D, Yi G S and Chow G M 2009 *J. Mater. Res.* **24** 2042
[26] Tian X, Wu Z, Jia Y, Chen J, Zheng R K, Zhang Y and Luo H 2013 *Appl. Phys. Lett.* **102** 42907
[27] Tikhomirov V K, Chibotaru L F, Saurel D, Gredin P, Mortier M and Moshchalkov V V 2009 *Nano. Lett.* **9** 721
[28] Schietinger S, Aichele T, Wang H Q, Nann T and Benson O 2010 *Nano Lett.* **10** 134
[29] Brites C D S, Lima P P, Silva N J O, Millán A, Amaral V S, Palacio F and Carlos L D 2010 *Adv. Mater.* **22** 4499
[30] Zhou J, Deng J, Zhu H, Chen X, Teng Y, Jia H, Xu S and Qiu J 2013 *J. Mater. Chem. C* **1** 8023
[31] Gainer C F, Joshua G S, De Silva C R and Romanowski M 2011 *J. Mater. Chem.* **21** 18530
[32] Gao D, Tian D, Xiao G, Chong B, Yu G and Pang Q 2015 *Opt. Lett.* **40** 3580
[33] Gao D, Zhang X, Chong B, Xiao G and Tian D 2017 *Phys. Chem. Chem. Phys.* **19** 4288
[34] Zhang S, Xu S, Ding J, Lu C, Jia T, Qiu J and Sun Z 2014 *Appl. Phys. Lett.* **104** 14101
[35] Zhang S, Yao Y, Xu S, Liu P, Ding J, Jia T, Qiu J and Sun Z 2015 *Sci. Rep.* **5** 13337
[36] Shang X, Chen P, Cheng W, Zhou K, Ma J, Feng D, Zhang S, Sun Z, Qiu J and Jia T 2014 *J. Appl. Phys.* **116** 063101
[37] Xu S, Yao Y, Lu C, Ding J, Jia T, Zhang S and Sun Z 2014 *Phys. Rev. A* **89** 053420
[38] Meshulach D and Silberberg Y 1998 *Nature* **396** 239
[39] Yao Y, Zhang S, Zhang H, Ding J, Jia T, Qiu J and Sun Z 2015 *Sci. Rep.* **4** 07295